Springer

KSME

Journal of Mechanical Science and Technology 28 (12) (2014) 5107~5115
www.springerlink.com/content/1738-494x
DOI 10.1007/s12206-014-1133-z

Research on the design of skiving tool for machining involute gears †

Erkuo Guo, Rongjing Hong*, Xiaodiao Huang and Chenggang Fang

Jiangsu Key Laboratory of Digital Manufacturing for Industrial Equipment and Control Technology, Nanjing Tech University, Nanjing, Jiangsu province, China

(Manuscript Received April 11, 2014; Revised August 14, 2014; Accepted August 21, 2014)

Abstract

Although the power skiving of gear process has demonstrated excellent capability in the latest research, the key to the successful application of skiving is the design of suitable tools. We propose a method to design and calculate the skiving tool for machining involute gears. First, according to the principle of power skiving for internal gear, the helical skiving cutter was designed with the modification coefficient and the tapered teeth that were oriented under a helix angle. The structure can avoid friction and interference, as well as ensure the even cutting load during the processing of skiving. Then, the kinematical model of power skiving was established and the profile of cutter with a rake angle was calculated based on the crossed helical gear engagement theory. Finally, using a helical cutter to simulate the machine for an internal spur gear, the results demonstrate that the proposed design method of skiving cutter can avoid interference and meet the requirement of power skiving.

Keywords: Power skiving; Involute gears; Skiving tool; Cutter design

1. Introduction

The power skiving process for machining internal gears is multiple times faster than shaping, and more flexible than broaching, due to skiving's continuous chip removal capability for the production of toothed gearings and rotational symmetrical parts with periodic structures. Although the patent for the skiving process was assigned in the beginning of the 20th century [1], the method was not implemented at that time because power skiving has always presented a challenge to machines and skiving tools. With the improvements in numerical control of direct drive technology, as well as the fast wear of uncoated cutters, the latest research demonstrates that power skiving is capable of being a highly productive and flexible alternative to the advanced technology in the market [2, 3].

The current developments were initiated at the Institute of Production Science (wbk) with the a numerical method to calculate the tools [4]. The subsequent methodical experimental analyses indicated the potential and advantages as mentioned above [5, 6]. Kobialka [7] considered power skiving as a contemporary gear pro-machining solution, and summarized the realization of power skiving, skiving tools and chip formation. Volker et al. [8] established a 3D-FEM model of gear skiving to investigate the kinematical conditions as well as chip formation mechanisms and evaluation of the effects on process reliability. Hartmut and Olaf [9] proposed a semi-completing skiving method and apparatus for gear power skiving. Then they provided a new method to improve the uniformity of load to both flank cutting edges and extend the longest possible tool service life [10].

Li and Chen et al. [11, 12] proposed a slicing technology for cylindrical gears to improve the limitation of current gear machining method for inner gear. Then Refs. [13, 14], a design method of error-free spur slice cutter was obtained; the structure of the rake face was determined according to technological realization of the design, manufacturing, and tool grinding. Although they laid a foundation for the study of spur cutter optimization and tool life, a more complex helical cutter for power skiving was not designed and calculated. Therefore, it is necessary to do some studies on the design theory and calculation method to meet the requirements of helical skiving tools of power skiving.

We propose a design method for helical skiving cutter of power skiving in gear manufacturing. According to the principle of power skiving for internal gear, the helical cutter is designed with positive modification coefficient and step-sharpened structure. Compared with the conventional design method, it could avoid interference, extend the working life of skiving cutter, as well as improve the uneven load during the processing of skiving. Then, the kinematical model of power skiving is established and the profile of cutter with a top rake angle is calculated. At last, using the designed skiving cutter

*Corresponding author. Tel.: +86 15850593351, Fax.: +86 02558132026
E-mail address: hongjmst@sina.com
† Recommended by Editor Haedo Jeong

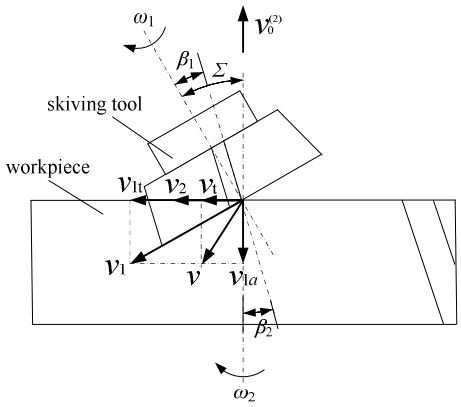

Fig. 1. Kinematical principle of power skiving.

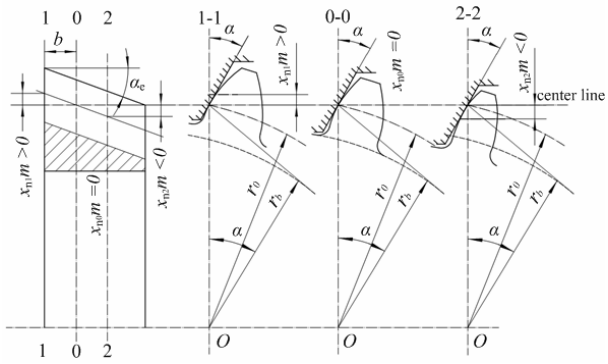

Fig. 2. Profile of skiving tool in different cross-section.

to simulate the machine of a spur gear, it clearly illustrates the feasibility of the proposed method.

2. Principle of gear power skiving process

Skiving is a continuous chip removal method for the production of toothed gearings. The process of power skiving is performed different from hobbing or sharping.

Fig. 1 shows the geometric setup of a skiving cutter relative to an internal ring gear; the top view shows internal helical gear with a shaft angle Σ between workpiece axes and skiving tool axes, and the shaft angle can be expressed as

$$\Sigma = \beta_1 \pm \beta_2 , \tag{1}$$

where β_1 is the helix angle of workpiece, β_2 is the helix angle of tool, the positive sign "+" indicates the helical screw of work and tool is opposite, the negative sign "-" indicates the helical screw of work and tool is identical.

According to the helical gear engagement theory of crossed axes, the cutting velocity in skiving is directly influenced by the speed of skiving tool v_1 and the workpiece v_2 and by the employed axis intersection angle Σ of the rotational axes. So the cutting velocity v results from the axial speed v_{1a} of skiving tool speed v_1 and the resultant speed v_t of work piece speed v_2 and tangential speed v_{1t}. In addition, there are further relative movements. The axial feed $v_0^{(2)}$ is required to be able to machine the entire gear tooth width using the tool.

Assume that the angular velocities of skiving tool and work piece are ω_1 and ω_2, respectively. Due to the influence of axial feed, the exact angular velocity of skiving tool should be performed by an incremental angular velocity $\Delta\omega_1$ with respect to ω_1. The incremental angular velocity of skiving tool, $\Delta\omega_1$ is determined by the following equation:

$$\Delta\omega_1 = \frac{2v_0^{(2)} \sin\beta_1}{m_n z_t} , \tag{2}$$

where $v_0^{(2)}$ is the axial feed of work piece, m_n is the normal module of tooth, z_t is the number of skiving tool.

Therefore, the relationship between the angular velocity of tool and workpiece and axial feed satisfies the following relation:

$$\omega_1 = \frac{z_g}{z_t}\omega_2 + \frac{2v_0^{(2)} \sin\beta_1}{m_n z_t} , \tag{3}$$

where z_g is the number of gears.

However, if the workpiece provides the increment movement, the relation can be represented as

$$\omega_2 = \frac{z_t}{z_g}\omega_1 - \frac{2v_0^{(2)} \sin\beta_1}{m_n z_g} . \tag{4}$$

3. The structure design for helical skiving tool

In skiving, manufacture and design errors of the skiving cutter will copy to the accuracy of gear, so the machining working accuracy mainly depends on the accuracy of skiving cutter design. Traditionally, power skiving is performed with common shaper cutters for machining involute helical gears. However, workpieces with spur teeth and large face width might cause interference between the slot and the far end of the cutting blade. The power skiving tools for spur gears working should be resharpened on the rake face and major flank. In this paper, we propose a novel design method for skiving cutter with a tapered teeth oriented under a helix angle.

3.1 The design for major flank of skiving cutter

To regrind the cutter after wearing and extend the tool life, a novel skiving cutter is designed with positive modification coefficient. For one thing, a modification coefficient is distributed to the teeth of skiving tools that can increase the versatility of skiving tools. For another thing, the top relief angle α_e and side relief angle α_0 are ground on major flanks; since the tooth thickness decreases from the top to the end in the direction of helix, it seems like a tapered skiving tool. As shown in Fig. 2, the tapered skiving tool is equal to helical gear with a big modification; the modification coefficients x_{n0},

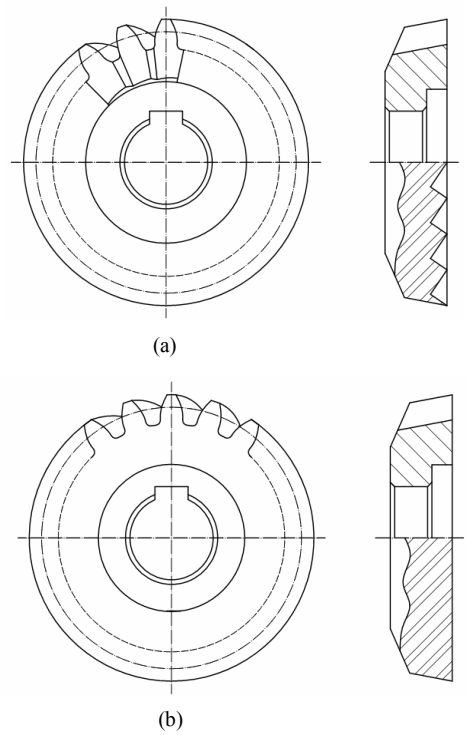

Fig. 3. (a) Novel skiving cutter; (b) conventional skiving cutter.

x_{n1}, x_{n2} are different from the cross-section: the farther from the front face, the less the modification coefficients. Sometimes, there is a zero cross-section in the middle of the cross-sections without modification coefficients.

3.2 The design for front face of skiving cutter

According to the gear principle, a cylindrical gear pair of helical gear is the conjugate tooth profile. Therefore, skiving cutter blades can be designed freely if those blades are on the conjugate tooth profile. However, to grind the cutter front face easily, the technology for manufacturing skiving cutter should be taken into account.

Compared with the conventional skiving cutter, the novel skiving cutter was designed as the tapered teeth oriented under a helix angle. In the traditional design, the cutter front face is oriented on the transverse plane (see Fig. 3(b)). Although it is easy to grind the front face, the side relief angles are unequal, which will lead to an uneven load during the process of power skiving and make it impossible to carry on the performance. Therefore, the cutter teeth of novel skiving cutter are projected with tapered teeth that the front face is oriented on the normal plane under a helix angle β (see Fig. 3(a)). The step-sharpened teeth cutter enables the same relief angles on both side flanks and avoids the interference between the skiving cutter rake face and gear tooth surface. Besides, to improve the machining condition of skiving cutter, a top rake angle γ is ground on the front face, see Fig. 4; the cutting angle definitions of a front face oriented on the normal plane are illustrated.

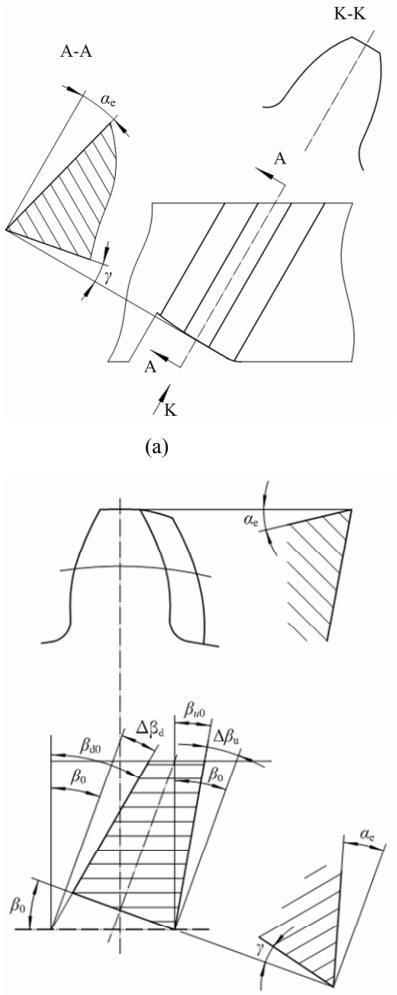

Fig. 4. Cutting angle definitions of a front face oriented on the normal plane: (a) grind method; (b) cutting angle definitions.

4. Calculation of skiving tool profile

4.1 Mathematical model of power skiving

Consider that Cartesian coordinate systems $\boldsymbol{S}(O\text{-}x,y,z)$ and $\boldsymbol{S_p}(O_p\text{-}x_p,y_p,z_p)$ are rigidly connected to the coordinate of skiving tool and coordinate of work piece, respectively (Fig. 5). The internal gear is oriented in the coordinate system $\boldsymbol{S_p}(O_p\text{-}x_p,y_p,z_p)$ with its axis of rotation collinear to the z_p-axes, and the skiving tool is oriented in the coordinate system $\boldsymbol{S}(O\text{-}x,y,z)$ with its axis of rotation collinear to the z-axes. The cutter center is positioned out of the center of z_p-y_p plane by a radial distance vector a.

As mentioned above, the angular velocity of skiving tool and work piece are $\boldsymbol{\omega}^{(1)}$ and $\boldsymbol{\omega}^{(2)}$, respectively. When the axial incremental movement O_2O_p is equal to l_2, the skiving tool rotates about z-axes by φ_1 and the work piece rotates about z_p-axes by φ_2. Using the homogeneous transformation matrix, the coordinate transformations can derive a simple representation

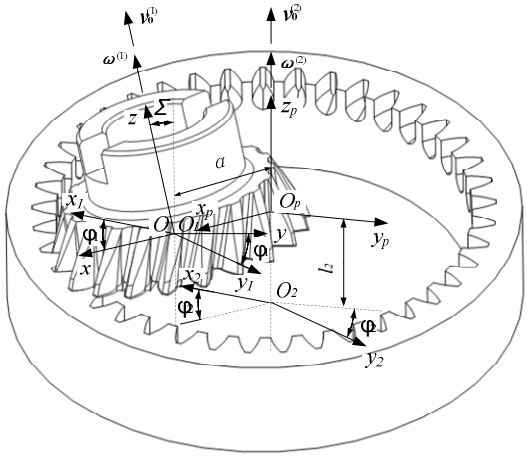

Fig. 5. Coordinate systems of power skiving.

of the relationship between the coordinate systems ***S(O-x,y,z)*** and ***S$_p$(O$_p$-x$_p$,y$_p$,z$_p$)*** by the 4×4 matrix

$$\begin{pmatrix} x_2 \\ y_2 \\ z_2 \\ t \end{pmatrix} = \mathbf{M}_{2p}\mathbf{M}_{p0}\mathbf{M}_{01}\begin{pmatrix} x_1 \\ y_1 \\ z_1 \\ t_1 \end{pmatrix} \tag{5}$$

where $\mathbf{M}_{01} = \begin{pmatrix} \cos\phi_1 & -\sin\phi_1 & 0 & 0 \\ \sin\phi_1 & \cos\phi_1 & 0 & 0 \\ 0 & 0 & 1 & 0 \\ 0 & 0 & 0 & 1 \end{pmatrix}$,

$\mathbf{M}_{2p} = \begin{pmatrix} \cos\phi_2 & -\sin\phi_2 & 0 & 0 \\ \sin\phi_2 & \cos\phi_2 & 0 & 0 \\ 0 & 0 & 1 & -l_2 \\ 0 & 0 & 0 & 1 \end{pmatrix}$,

$\mathbf{M}_{p0} = \begin{pmatrix} 1 & 0 & 0 & a \\ 0 & \cos\Sigma & -\sin\Sigma & 0 \\ 0 & -\sin\Sigma & \cos\Sigma & 0 \\ 0 & 0 & 0 & 1 \end{pmatrix}$.

4.2 The equation of meshing

Skiving process can be investigated as a pair of helical crossed gear engagement; tool surface and gear tooth surface are designated as $\Sigma^{(1)}$ and $\Sigma^{(2)}$, respectively. So the tool profile should satisfy the equation of meshing [10, 11]

$$\mathbf{v}^{(12)} \cdot \mathbf{n} = 0 . \tag{6}$$

Consider that the tool surface is represented by the vector equation

$$\mathbf{r}^{(1)} = \mathbf{r}^{(1)}(u,\theta) = x_1(u,\theta)\mathbf{i} + y_1(u,\theta)\mathbf{j} + z_1(u,\theta,p)\mathbf{k} , \tag{7}$$

where (u,θ) are the surface parameters; p is the screw parameter in the screw motion about the z axis. The normal to the surface is represented as

$$\mathbf{n}^{(1)} = \frac{\partial \mathbf{r}^{(1)}}{\partial u} \times \frac{\partial \mathbf{r}^{(1)}}{\partial \theta} = \begin{vmatrix} \mathbf{i}_1 & \mathbf{j}_1 & \mathbf{k}_1 \\ \dfrac{\partial x_1}{\partial u} & \dfrac{\partial y_1}{\partial u} & \dfrac{\partial z_1}{\partial u} \\ \dfrac{\partial x_1}{\partial \theta} & \dfrac{\partial y_1}{\partial \theta} & \dfrac{\partial z_1}{\partial \theta} \end{vmatrix} = n_{x_1}^{(1)}\mathbf{i}_1 + n_{y_1}^{(1)}\mathbf{j}_1 + n_{z_1}^{(1)}\mathbf{k}_1 . \tag{8}$$

According to the principle of gearing, the angular velocity and the axial feed are independent with a two-degree of freedom engagement movement. Thus, the meshing equation is represented as follows [10]:

$$U_1 \cos\phi_1 - V_1 \sin\phi_1 = W_1 \tag{9}$$

$$U_2 \cos\phi_1 - V_2 \sin\phi_1 = W_2 \tag{10}$$

where $\begin{cases} U_1 = i_{21}\left(-z_1 n_{x_1}^{(1)} \sin\Sigma - a n_{y_1}^{(1)} \cos\Sigma + x_1 n_{z_1}^{(1)} \sin\Sigma\right) \\ V_1 = i_{21}\left(-z_1 n_{y_1}^{(1)} \sin\Sigma + a n_{x_1}^{(1)} \cos\Sigma + y_1 n_{z_1}^{(1)} \sin\Sigma\right) \\ W_1 = \left(1 - i_{21}\cos\Sigma\right)\left(y_1 n_{x_1}^{(1)} - x_1 n_{y_1}^{(1)}\right) - a i_{12} n_{z_1}^{(1)} \sin\Sigma \end{cases}$,

$\begin{cases} U_2 = i''\left(-z_1 n_{x_1}^{(1)} \sin\Sigma - a n_{y_1}^{(1)} \cos\Sigma + x_1 n_{z_1}^{(1)} \sin\Sigma\right) - n_{y_1}^{(1)} \sin\Sigma \\ V_2 = i''\left(-z_1 n_{y_1}^{(1)} \sin\Sigma + a n_{x_1}^{(1)} \cos\Sigma + y_1 n_{z_1}^{(1)} \sin\Sigma\right) + n_{x_1}^{(1)} \sin\Sigma \\ W_2 = -i''\left(y_1 n_{x_1}^{(1)} - x_1 n_{y_1}^{(1)}\right)\cos\Sigma + \left(\cos\Sigma - a i'' \sin\Sigma\right) n_{z_1}^{(1)} \end{cases}$,

whereby i_{21} indicates the ratio between skiving tool and workpiece, $i'' = \dfrac{2\sin\beta_2}{m_n z_g}$.

When the angle φ_1 is given, one solution (u,θ) meets the requirements of both Eqs. (9) and (10). Eqs. (7)-(10), yield

$$\frac{y_1 n_{x_1}^{(1)} - x_1 n_{y_1}^{(1)}}{i_{21}} - \frac{n_{z_1}^{(1)} \cos\Sigma + n_{y_1}^{(1)} \sin\Sigma \cos\phi_1 + n_{x_1}^{(1)} \sin\Sigma \sin\phi_1}{i''} = 0 . \tag{11}$$

4.3 Equations of tooth profile

Equations of the gear tooth profile in transverse plane are represented as

$$\begin{cases} x_0 = r_b \cos(\sigma_0 + u) + r_b u \sin(\sigma_0 + u) \\ y_0 = r_b \sin(\sigma_0 + u) - r_b u \cos(\sigma_0 + u) \end{cases} , \tag{12}$$

where r_b is the radius of base circle, σ_0 is the half of angular tooth thickness on the base circle.

The normal to the transverse tooth profile is

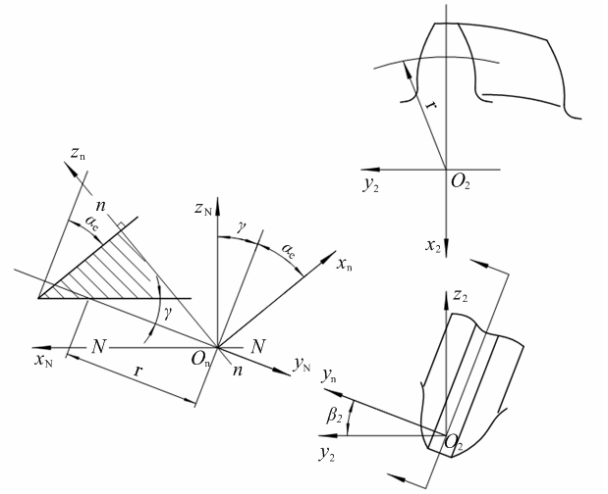

Fig. 6. The normal cutting blade.

$$\begin{cases} x_0' = r_b \cos(\sigma_0 + u) \\ y_0' = r_b \sin(\sigma_0 + u) \end{cases}. \tag{13}$$

Using the coordinate transformation from $\boldsymbol{S_p}$ to $\boldsymbol{S}$, we obtain the tooth profile by the equations

$$\begin{cases} x_1 = x_0 \cos(\theta + \phi_2) + y_0 \sin(\theta + \phi_2) \\ y_1 = x_0 \sin(\theta + \phi_2) - y_0 \cos(\theta + \phi_2) \\ z_1 = p(\theta + \phi_2) \end{cases}, \tag{14}$$

where φ_2 is the rotation angle of work piece.

Similarly, the tooth profile is obtained in the coordinate system of skiving tool by the following equations:

$$\begin{cases} x_2 = (x_1 \cos\phi_1 - y_1 \sin\phi_1 + a)\cos\phi_2 \\ \quad +\left[(x_1 \sin\phi_1 + y_1 \cos\phi_1)\cos\Sigma - z_1 \sin\Sigma)\right]\sin\phi_2 \\ y_2 = -(x_1 \cos\phi_1 - y_1 \sin\phi_1 + a)\sin\phi_2 \\ \quad +\left[(x_1 \sin\phi_1 + y_1 \cos\phi_1)\cos\Sigma - z_1 \sin\Sigma)\right]\cos\phi_2 \\ z_2 = (x_1 \sin\phi_1 + y_1 \cos\phi_1)\sin\Sigma + z_1 \cos\Sigma - l_2 \end{cases} \tag{15}$$

where φ_1 is the rotation angle of the contact point that satisfies the meshing equation.

4.4 Equations of cutting blade in normal plane

Due to the top rake angle γ on the front face of skiving cutter, the cutting blade on the front face can be calculated by

$$(x_2 + r)\tan\gamma + y_2 \sin\beta_2 - z_2 \cos\beta_2 = 0, \tag{16}$$

where r is the radius of skiving tool in pitch circle, β_2 is the helix angle of skiving tool, γ is the rake angle.

Eqs. (11), (15) and (16) yield the cutter blade

$$\begin{cases} x_2 = (x_1 \cos\phi_1 - y_1 \sin\phi_1 + a)\cos\phi_2 \\ \quad +\left[(x_1 \sin\phi_1 + y_1 \cos\phi_1)\cos\Sigma - z_1 \sin\Sigma)\right]\sin\phi_2 \\ y_2 = -(x_1 \cos\phi_1 - y_1 \sin\phi_1 + a)\sin\phi_2 \\ \quad +\left[(x_1 \sin\phi_1 + y_1 \cos\phi_1)\cos\Sigma - z_1 \sin\Sigma)\right]\cos\phi_2 \\ z_2 = (x_1 \sin\phi_1 + y_1 \cos\phi_1)\sin\Sigma + z_1 \cos\Sigma - l_2 \\ (x_2 + r)\tan\gamma + y_2 \sin\beta_2 - z_2 \cos\beta_2 = 0 \\ \dfrac{y_1 n_{x_1}^{(1)} - x_1 n_{y_1}^{(1)}}{i_{21}} - \dfrac{n_{z_1}^{(1)} \cos\Sigma + n_{y_1}^{(1)} \sin\Sigma \cos\phi_1 + n_{x_1}^{(1)} \sin\Sigma \sin\phi_1}{i''} = 0 \end{cases}. \tag{17}$$

According to the meshing Eq. (11), x_0', y_0', $n_{x_1}^{(1)}$, $n_{y_1}^{(1)}$, and $n_{z_1}^{(1)}$ are related to the parameters u, and p, Σ, i'', and i_{21} are constant. Therefore, assuming that u is equal to $(\theta+\varphi_1)$, we can solve the parameter u.

$$\theta = n_{z_1}^{(1)} \left(\frac{\left[x_0 \cos(\theta + \phi_1) - y_0 \sin(\theta + \phi_1)\right]\sin\Sigma}{p^2\left[x_0' \sin(\theta + \phi_1) + y_0' \cos(\theta + \phi_1)\right]\sin\Sigma} - \frac{\Sigma\left(\dfrac{1}{i_{21}} - \cos \quad p\dfrac{ai''\cot\Sigma}{i_{21}}\right) + \dfrac{a}{\sin\Sigma}}{p^2\left[x_0' \sin(\theta + \phi_1) + y_0' \cos(\theta + \phi_1)\right]\sin\Sigma} \right). \tag{18}$$

Then, substituting Eq. (11) into Eq. (9), Eq. (10) yields the tooth parameter θ, that is $\theta = \theta(u)$, so the rotation angle φ_1 can be derived by subtracting θ form $(\theta+\varphi_1)$. Consequently, we obtain the cutter blade equations by substituting the parameters u, θ, and φ_1 into Eq. (17).

To facilitate manufacturing and measuring for the cutter profile, the normal cutting blade not only parallel to the front face, but perpendicular to the direction of cutter surface, should be calculated. The normal cutter profile in the section of N-N is represented as

$$\begin{cases} x_N = -x_2 \cos\gamma + y_2 \sin\gamma \sin\beta_2 - z_2 \sin\gamma \cos\beta_2 \\ y_N = y_2 \cos\beta_2 + z_2 \sin\beta_2 \end{cases}. \tag{19}$$

4.5 The correction for the pressure angle of cutter blade

In this method, due to the top rake angle γ on the front face, the gear worked by this cutter will result in tooth error. However, we provide a method, by correcting the pressure angle of cutter profile, to eliminate the error.

Actually, the power skiving cutter can be viewed as the helical gear with a modification coefficient that engages a modified gear rack. Thus, the angles on the gear rack are considered as the angles on the skiving cutter. To simplify the calculation, the angles on the skiving cutter can be derived from the geometric properties performed on the gear rack. Taking a modification helical gear rack for example, we obtain the corrected cutter blade.

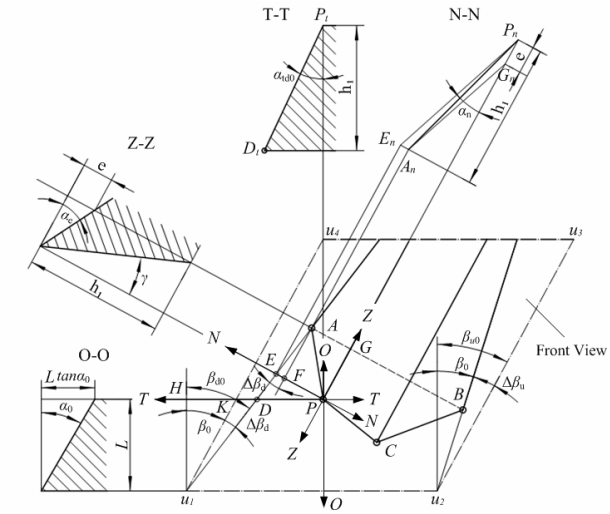

Fig. 7. Front view of cutting angles for a modified helical gear rack.

As shown in Fig. 7, the cross-section $u_1u_2u_3u_4$ is the part of gear rack top tooth; all the angles on the plane $u_1u_2u_3u_4$ with respect to gear rack are equal to those angles on skiving cutter. For instance, the helix angle β on gear rack is equal to the helix angle in the cylindrical circle on skiving cutter; $\Delta\beta_d$ and $\Delta\beta_u$ are the side rake angle of skiving cutter, AP, BC, and PC are the side cutting blades and top cutting blade, respectively. Besides, γ and α_e on the longitudinal section Z-Z are the top rake angle and top relief angle; the projection angle α_n on the normal section N-N equals the normal pressure angle, and the pressure angle α_{td0} on the transverse section T-T is equal to the corrected pressure angle in the left of the skiving cutter.

In view of geometry relation of Fig. 7, the side relief angle $\Delta\beta_d$ on the left of skiving cutter can be expressed as

$$\tan\Delta\beta_d = \frac{EF}{AF} = \frac{EP-FP}{AF} = \frac{\frac{EP}{h_1}-\frac{FP}{h_1}}{\frac{AF}{h_1}} = \frac{\frac{FP}{h_1-e}-\tan\alpha_n}{\tan\gamma}. \tag{20}$$

Substituting the given equation $e = AF\tan\alpha_e$, yields

$$\tan\Delta\beta_d = \frac{\tan\alpha_n\tan\alpha_e}{1-\tan\gamma\tan\alpha_e}. \tag{21}$$

Similarly, the side relief angle $\Delta\beta_u$ on the right is expressed as

$$\tan\Delta\beta_u = \frac{\tan\alpha_n\tan\alpha_e}{1-\tan\gamma\tan\alpha_e}. \tag{22}$$

As a result, $\Delta\beta_d = \Delta\beta_u = \Delta\beta$, that is the side relief angles on both flanks are the same, thus

$$\tan\Delta\beta = \frac{\tan\alpha_n\tan\alpha_e}{1-\tan\gamma\tan\alpha_e} = \frac{\tan\alpha_n}{\cot\alpha_e-\tan\gamma}. \tag{23}$$

The helix angle of skiving cutter on both sides can be represented as

$$\begin{cases}\beta_{d0} = \beta+\Delta\beta\\ \beta_{u0} = \beta-\Delta\beta\end{cases}. \tag{24}$$

According to the top view of the cutting angles illustration, the helix angle β_{d0} on left flank is represented as

$$\tan\beta_{d0} = \frac{DH}{L} = \frac{DK+KH}{L} = \tan\beta+\frac{DK}{L}. \tag{25}$$

It is easy to obtain the relation on the cross-section O-O and T-T

$$DK = L\tan\alpha_0\tan\alpha_{td0}. \tag{26}$$

Substituting Eq. (21) into Eq. (20), yields

$$\tan\beta_{d0} = \tan\beta+\tan\alpha_0\tan\alpha_{td0}. \tag{27}$$

Consequently, the corrected pressure angle α_{td0} and α_{tu0} on the right and left flank of skiving cutter are presented as

$$\begin{cases}\alpha_{td0} = a\tan\left(\dfrac{\tan\beta_{d0}-\tan\beta}{\tan\alpha_0}\right) = a\tan\left(\dfrac{\tan(\beta+\Delta\beta)-\tan\beta}{\tan\alpha_0}\right)\\ \alpha_{tu0} = a\tan\left(\dfrac{\tan\beta-\tan\beta_{u0}}{\tan\alpha_0}\right) = a\tan\left(\dfrac{\tan\beta-\tan(\beta-\Delta\beta)}{\tan\alpha_0}\right)\end{cases} \tag{28}$$

where $\Delta\beta = a\tan\left(\dfrac{\tan\alpha_n}{\cot\alpha_e-\tan\gamma}\right)$.

Eq. (28) indicates that the corrected pressure angle is related to the normal pressure angle α_n, the helix angle β, the top rake angle γ and top relief angle α_e.

5. Numerical example and simulation

To verify the accuracy of the cutter profile and the validity of avoid inference, a numerical example that illustrates our proposed design method is based on machining the internal spur gear by numerical calculation and simulation.

According to the given parameters of internal helical gear and the proposed calculation method, basic parameters of skiving cutter can be derived in the numerical example, as listed in Table 1.

To investigate the effects of pressure angle correction on the skiving cutter profile, we derive the pressure angle after correction and the cutter profile deviation after correcting pressure angle in Figs. 8 and 9, respectively.

Table 1. Basic parameters of workpiece and cutter in the example.

Items		Value
Teeth number of gear	z_g	57
Normal module (mm)	m_n	3
Pressure angle (deg)	α_n	20
Helix angle (deg)	β	20
Teeth number of cutter	z_t	21
modification of cutter	x_n	0.23
Rake angle of cutter (deg)	α_e	4
Top side relief angle of cutter (deg)	γ	10
Flank side relief angle of cutter (deg)	α_{td0}	17.26

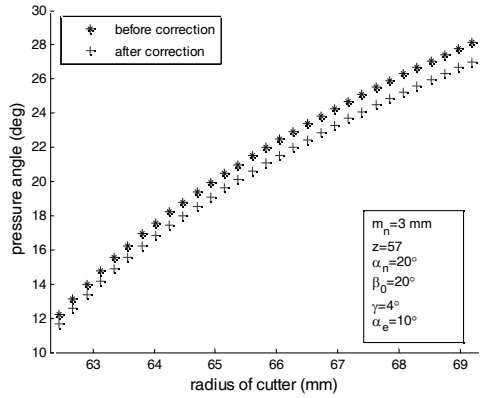

Fig. 8. Pressure angle before and after correction.

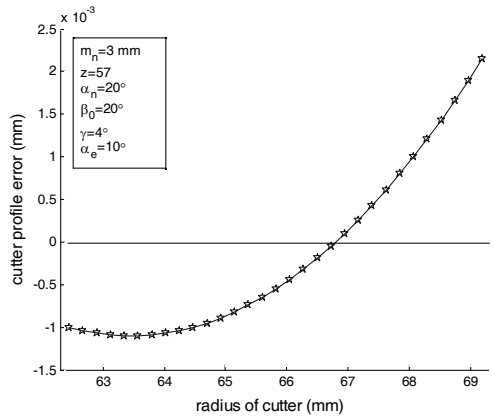

Fig. 9. Cutter profile deviation after correct pressure angle.

As Fig. 8 shows, the pressure angle after correction is less than that before correction with the change of cutter radius, which explains the influence of flank side relief angle. Fig. 9 presents the cutter profile deviation after calculating and correcting of pressure angle. Although the cutter profile deviation is $+2.5\times10^{-3}$ mm in the top of cutter 69.2 mm and -1.1×10^{-3} mm in the bottom of cutter 62.1 mm, the cutter profile deviations are less than 2.5×10^{-3} mm on the entire cutting blade so the deviations can be neglected with respect to the machining error.

Fig. 10 illustrates the design of skiving cutter including a

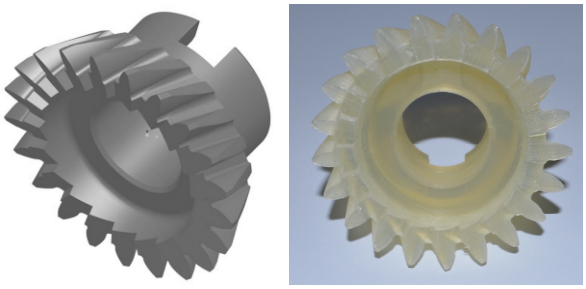

(a) (b)

Fig. 10. Design of skiving cutter: (a) 3D modeling; (b) skiving cutter by 3D printer.

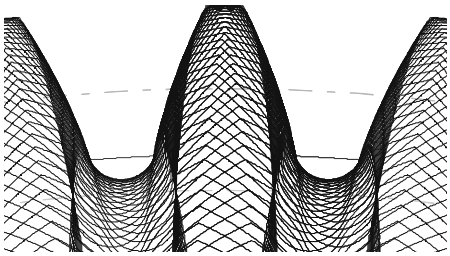

Fig. 11. Tooth profile performed by the design skiving cutter.

3D model and a skiving cutter by 3D printer. First, establish the 3D CAD model with the designed cutter parameters by the proposed method. Then, save the 3D CAD model as the data file format of stereo lithographic (stl). Finally, with the help of 3D printer, the complicated skiving cutter is available.

To verify the working accuracy of the design skiving cutter, Figs. 11 and 12 show the tooth profile performed by the design skiving cutter and the simulation of power skiving separately. The simulated flank topographic gear errors produced by the skiving process can be obtained using the software. As Fig. 12 illustrates, the tooth deviation on the overcut area is less than -2.4×10^{-3} mm and on the residual area is less than 2.1×10^{-3} mm.

In this example, the simulated flank theoretical errors with the change of cutter and workpiece parameters are given in Fig. 13. The flank theoretical errors increase with increasing cutter rake angle and relief, workpiece helix angle and normal module. However, the maximum theoretical error is less than 3.5×10^{-3} mm in a common range of workpiece and cutter parameters. Obviously, the theoretical error is small enough that it can be neglected in gear manufacturing and the design cutter can satisfy the needs of skiving. The simulated results demonstrate that the proposed design method of skiving cutter can avoid interference and meet the requirement of power skiving.

6. Conclusions

We have proposed a method to design and calculate the skiving tool for machining involute gears. We established the kinematical model of power skiving and calculated the profile

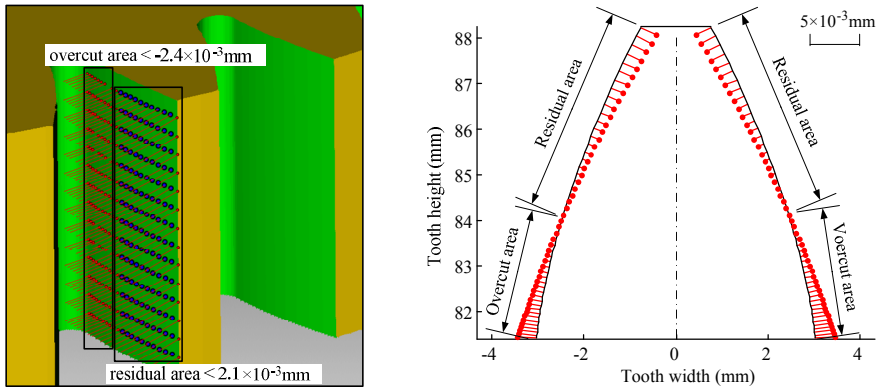

(a) (b)

Fig. 12. Simulated tooth deviations on tooth flank by the design skiving cutter: (a) simulation; (b) tooth deviations on tooth profile.

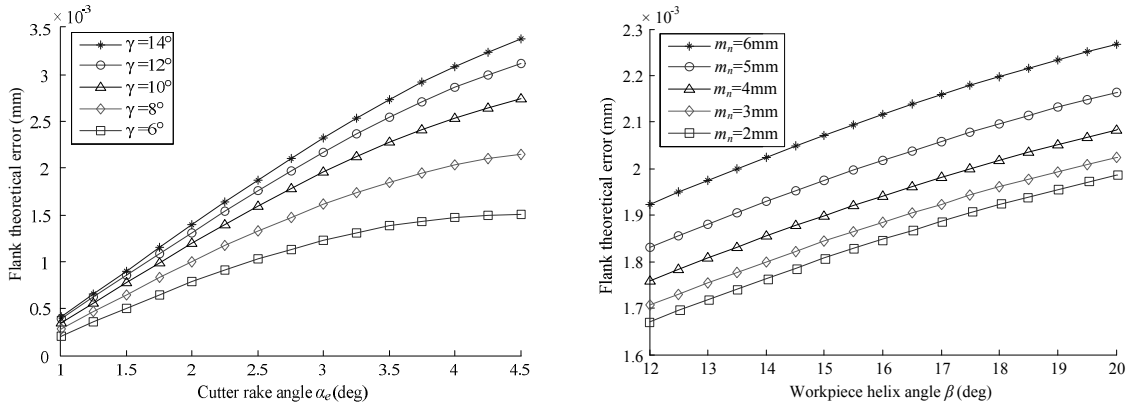

(a) (b)

Fig. 13. Simulated flank theoretical errors by the design skiving cutter: (a) change of cutter rake angle and relief angle; (b) change of workpiece helix angle and normal module.

of cutter with a rake angle based on the crossed helical gear engagement theory. Compared with the conventional design method, the skiving cutter was designed with the modification coefficient and the tapered teeth that were oriented under a helix angle, which could avoid interference, extend the working life of skiving cutter, as well as improve the uneven load during the processing of skiving. A numerical example was given and discussed; it demonstrated the novel design method for skiving cutter can meet the requirement of power skiving and increase the process capability of cutter manufacturing. Future studies will be directed to exploring the following aspects, such as the testing of cutting performance by extensive experiments, the versatility of helical skiving cutter, and the design of skiving cutter for non-involute helical gear.

Acknowledgment

This work supported by the National Natural Science Foundation (No.51175242), China.

Nomenclature

Σ	: Shaft angle between workpiece axes and tool axes
β	: Helix angle
β_1	: Helix angle of workpiece
β_2	: Helix angle of skiving tool
$\boldsymbol{v}$	: Cutting velocity
$\boldsymbol{v}_1$	: Speed of skiving tool
$\boldsymbol{v}_2$	: Speed of workpiece
$\boldsymbol{v}_{1a}$	: Axial speed of skiving tool
$\boldsymbol{v}_{1t}$	: Tangential speed of workpiece
$\boldsymbol{v}_t$	: Resultant speed of $\boldsymbol{v}_2$ and $\boldsymbol{v}_{1t}$
$\boldsymbol{v}_0^{(2)}$	: Axial feed of workpiece
ω_1	: Angular velocity of skiving tool
ω_2	: Angular velocity of workpiece
$\Delta\omega_1$	: Incremental angular velocity with respect to ω_1
m_n	: Normal module of teeth
z_t	: Number of skiving tool teeth
z_g	: Number of gear teeth
i_{21}	: Ratio between skiving tool and workpiece

$x_{n0,1,2}$: Modification coefficients
α_e : Top relief angle
α_0 : Side relief angle
γ : Rake angle on the front face
a : Radial distance between workpiece and tool axes
l_2 : Axial incremental movement
φ_1, φ_2 : Rotation angles about z-axes
u,θ : Surface parameters
p : Screw parameter
r_b : Radius of base circle
σ_0 : Half angular tooth thickness on the base circle
α_n : Projection of pressure angle
$\Delta\beta_d$: Right side rake angle
$\Delta\beta_u$: Left side rake angle
α_{td0} : Right corrected pressure angle
α_{tu0} : Left corrected pressure angle

References

[1] J. Jin, The principle of gear turning and experimental results, *Xi'an Jiaotong University*, 2 (1962) 69-97.

[2] J. Kreschel, *Gleason power skiving: technology and basics*, Gleason Company Publication, Ludwigsburg, Germany (2012).

[3] H. Stadtfeld, Power skiving of cylindrical gears on different machine platforms, *Gear Technology*, 31 (1) (2014) 52-62.

[4] D. Spath and A. Huhsam, Skiving for high-performance machining of periodic structures, *Annals of the CIRP*, 51 (1) (2002).

[5] J. Fleischer, A. Bechle and C. Kuhlewein, Process development of skiving-a highly productive gearing process, *CIRP January Meeting, Presentation STC-C*, Paris (2006).

[6] J. Fleischer, A. Bechle and C. Kuhlewein, High performance gearing by skiving, *CIRP 2nd International Conference on High Performance Cutting (HPC)*, June 12th -13th, University of British Columbia, Vancouver, Canada (2006).

[7] C. Kobialka, Contemporary gear pre-machining solutions, *AGMA No.12, FTM11, ISBN: 987-1-61481-042-1* (2012).

[8] S. Volker, K. Chirstoph and A. Hermann, 3D-FEM modeling of gear skiving to investigate and chip formation mechanisms, *Advanced Materials Research*, 223 (2011) 46-55.

[9] M. Hartmut and V. Olaf, Robust method for skiving and corresponding apparatus comprising a skiving tool, US, *Patent, 201203283844A* (2012).

[10] M. Hartmut and V. Olaf, Semi-completing skiving method and device having corresponding skiving tool for executing a semi-completing skiving method, US, *Patent, 2013007119741* (2013).

[11] J. Li, X. C. Chen and H. Y. Zhang, Slicing technology for cylindrical gears, *Chinese J. of Mechanical Engineering*, 47 (19) (2011) 193-198.

[12] X. C. Chen, J. Li and B. C. Lou, A study on the design of error-free spur slice cutter, *The International J. of Advanced Manufacturing Technology*, 68 (2013) 727-738.

[13] X. C. Chen, J. Li and B. C. Lou, Effect of the cutter parameters and machining parameters on the interference in gear slicing, *Chinese J. of Mechanical Engineering*, 26 (6) (2013) 1118-1126.

[14] X. C. Chen et. al., A study on the grinding of the major flank face of error-free spur slice cutter, *The International J. of Advanced Manufacturing Technology*, 2 (2014).

[15] X. T. Wu, *Principle of gearing*, 2nd ed. Xi'an Jiaotong University Press, Xi'an (2009).

[16] F. L. Litvin and A. Fuentes, *Gear geometry and applied theory*, 2nd ed. Cambridge University Press, New York (2004).

Rongjing Hong received his Ph.D. from Southeast University, China, in 2006. He is currently a professor at the School of Mechanical and Power Engineering, Nanjing Tech University. His research interests are in advanced CNC technology and the mechanical vibration theory.

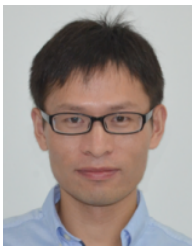

Erkuo Guo received his M.S. degree from Nanjing Tech University, China, in 2013. He is currently a Ph.D. candidate at Nanjing Tech University. His research interests are in advanced CNC technology and gear equipment and advanced manufacturing engineering.